COMPUTATIONAL STUDY ON THE EFFECT OF INJECTION STRATIFICATION SEQUENCE ON DIESEL IC ENGINE EMISSIONS OF SOOT AND NO_X

Fernando Lopez-Parra
General Electric Company Polska

Abstract

The work contained in this paper represents the final stage of the PhD project, where the findings from the free-jet flames were applied to a typical Diesel IC engine in order to investigate whether a similar outcome was feasible.

For this part of the research, a computational study on the effect of staggered fuel injection in a direct injection diesel engine is performed. This work is aimed at exploring the practical applications of previous work by the authors, where simultaneous soot and NO_x abatement was achieved in turbulent diffusion flames by means of pulsing the fuel stream. The soot model employed in this investigation is based on the Eddy Dissipation Concept of Magnussen, which represents a reasonable intermediate step between the empirical and the phenomenological models, as it accounts for the effects of small scale turbulence in soot formation and combustion, but does not rely on multi-step reaction mechanisms. The results hereby presented aim to capture realistic soot formation trends that are based on real physical phenomena and, hence, serve as a stepping stone for more specific development work.

The geometry was based on a simplified, 60-degree section of a valve-less Caterpillar 3406 single cylinder heavy-duty engine. The RNG k-ε model was employed to solve for the turbulence field and the main reaction chemistry was solved with a single-step gasoil-air mechanism, whereas the Eddy Dissipation Concept was employed to predict the turbulence-chemistry interaction and the Discrete Ordinates model used for radiation.

The results showed that there is a strong interaction between the pulse sequence and combustion development, although it is difficult to judge whether these differences are due to the dwell between the first two pulses of any sequence or the sequence itself.

A 4-pulse injection sequence predicted reduced soot emissions, albeit maintaining higher in-cylinder temperatures during the expansion stroke, which increased the NO_x production. The investigation was performed at two engine regimes: 1600 and 2300rpm, with some significant differences in the flame structure and development seen between these.

1. INTRODUCTION

The ever rising cost of fuel and the fears of climate change are encouraging many of the automotive manufacturers to dedicate a significant amount of time and resources to the investigation of fuel efficiency and pollutant emissions, as there are growing concerns about the effects that the presence of pollutants such as soot and NO_x in the atmosphere [1], [2]. In addition, the study of internal combustion engines through computational simulation is also gaining a number

of converts in the field, as the accuracy and the computational power are reaching reasonable level of robustness and the difficulties and limitations encountered in the empirical process are managed.

In the field of diesel engines, Computational Fluid Dynamics (CFD) has helped to understand the phenomena taking place during combustion and, as a result, to improve the entire design process in diesel IC engines. As the diesel engine assumes a more visible standing within the transportation industry, it is important to eliminate the generalized perception that these are heavy polluters and the engines provide very slow response.

In addition to the pollutant emissions issue, the diesel industry must also ensure that the overall performance of these engines is on a par with their petrol counterparts. In general, most diesel engine manufacturers choose injection advancements that are in the region of 10 crank angle degrees (CAD), which normally allows the combustion to start just before the top dead centre (TDC). As a result, the maximum pressure achieved during the cycle is much higher. On the other hand, this performance increase normally comes at the cost of higher emission levels, mainly due to pressure effects in the thermodynamics of the combustion process and, hence, on the pollutant emission levels. In most cases, modern technology has alleviated this problem by enabling us to run much higher injection pressures, which would effectively reduce the Sauter Mean Diameter (SMD) of the droplet size distribution. However, this is still insufficient to satisfy the emissions regulations, as they become more and more stringent.

The scope for improvements in diesel engine technology is reasonably wide, and techniques such as increments in injection pressure [3], inlet valve lift profiles [4] and fuel composition effects [5] have been investigated recently. In addition to these, one of the most active investigation lines is the stratified charge injection, although the data publicly available is limited in this area.. The primary objective of this technique is to increase inasmuch as possible the portion of the combustion that takes place in a premixed-like condition. This would be achieved by generating a series of pulses with a small amount of fuel that would be able to vaporize very quickly, as the droplets are injected directly into a reacting zone with high temperatures and the reduced size of the spray prevents the formation of a fuel rich core, an area where a large portion of the particulates are formed. The pulse sequences that have been simulated in the present work constitute the preliminary stages for additional work. Here we will look at the effect of using square pulses in four different patterns: 4 (modes A and B), 8 and 14 pulses. The difference between modes A and B is the dwell between the injection pulses, as depicted in figure 1. The injection sequences that have been tested in the present work are all based in an advanced Start of Injection (SOI) and maintain the duration of the injection for all cases, apart from the 4-pulse type B, which had lower dwells between pulses.

Previous work done by Reitz and Rutland [6] suggest that one of the main parameters that can be modified in order to control the level of pollutant emissions is the lapse between the first and the second injection pulses. In the current case study, this parameter was only tackled in an indirect manner, as the different injection sequences were designed with a fixed SOI and constant fuel flow rate and injection duration.

2. PROBLEM DESCRIPTION AND METHODOLOGY

The geometry and approach used in this case study is based on a Caterpillar single cylinder heavy duty engine, on which a significant amount of computational work has been done in the past in order to investigate droplet evaporation[7] and chemistry models [8], [9]. Whereas the use of detailed models for chemistry, such as multiple flamelets [10], [11] and soot [12], [13] are rigorously required for quantitative accuracy, these proved computationally to be very expensive considering the objective of the current work. The design characteristics and specification, as they were used in the CFD solver are detailed in table 1. The flow domain is formed by a 60-degree section of the cylinder, since the valves were not simulated and a 6-nozzle injector was employed.

Table 1. Direct injection diesel engine characteristics

Cylinder bore x stroke (mm)	137.6 x 165.1
Connecting rod length (mm)	261.62
Inlet valve diameter (mm)	46.3
Exhaust valve diameter (mm)	43.9
Displacement volume (L)	2.44
Compression ratio	15.1
Piston crown	Mexican hat
Inlet air pressure (kPa)	174.325
Inlet air temperature (K)	310
Intake valve closure (CAD)	-147 ATDC
Engine speed (rpm)	1668 / 2300

In general, the detailed data necessary to define the boundary conditions fully are rarely available, hence the average droplet size in the spray were deduced from the work of Sirignano [14] and Ahn *et al.* [15]. The injection spray was simulated as a solid cone spray of particles of 25μm SMD and Rosin-Rammler distribution. An injection period of 21 CAD and the total fuel mass flow was kept consistent throughout the case study. Injection sequences of 4, 8 and 14 pulses were simulated and compared to the baseline single pulse.

The soot model employed in the current work was implemented in the CFD solver via a user-defined source routine . Like the turbulence-chemistry interaction, this model was based on the Eddy Dissipation concept of Magnussen [16]. The advantages of this soot model compared to simpler models [17, 18] refer to the ability to account for turbulence effects in the formation and combustion rates of the soot particulates. This is achieved by the inclusion of the concept of fine structures, which can analogously be described as thin vortex sheets or tubes of characteristic length equal to the Kolmogorov microscales [19, 20]. The molecular mixing, and hence the reaction, occurs within these fine structures, causing as a result, an increase of the local temperature with respect to the fluid outside these vortex structures; and the mass fraction occupied by these fine structures is strongly coupled to the turbulence intensity and dissipation rate, as described in equation 1. In general, the average soot particle size can be computed from flame data following the methodology described in the work of Magnussen [21, 22].

$$\gamma^* = 9.7 \cdot \left(\frac{\nu \cdot \varepsilon}{k^2} \right)^{0.75} \tag{1}$$

The net formation of soot was broken down into two differentiated stages: nucleation and soot inception; a transport equation was solved for each one of these. Given the subtleties of IC engine modelling in its own right, the soot model employed was chosen on the basis of relative simplicity, whilst taking into account the effects of turbulence in the formation and combustion of soot particulates. The current case study assumes a monodisperse soot particle size distribution with an average soot particle size of 0.05μm; hence, it is not the purpose of this study to compete with more detailed soot models with variable soot size distribution [23]. The transport equations solved for the formation of nuclei and soot are given in equations 2 and 3 respectively, where * and o indicate fine structures and surrounding fluid respectively. A more detailed description and discussion of these can be found in previous works by the authors [24, 25].

$$R_{n,f} = \left(n_o^* \frac{\gamma^* \chi}{\rho^*} + n_o^o \frac{1-\gamma^* \chi}{\rho^o} + g_o n^* \frac{\gamma^* \chi}{\rho^*} \left(N^o - N^* \right) \right) \rho + \\ + (f-g) \rho Y_{mic} - g_o \rho N^o Y_{mic} \tag{2}$$

$$R_{s,f} = m_p\left(a\rho Y_{nuc} + b\rho N^* \frac{\gamma^* \chi}{\rho^*}\left(n^o - n^*\right)\right) - bn^o \rho Y_{soot} \tag{3}$$

where χ is the fraction of fine structures that are heated sufficiently to react; n_o is the spontaneous rate of nuclei formation and N is the concentration of soot particles. Y_{nuc} and Y_{soot} refer to the mass fractions of nuclei and soot respectively; and they are the scalars computed in the soot model. The remaining parameters are model constants that assigned values as described in table 2 [26].

Table 2. Constants employed in the soot model

g_o	1e-15	m^3/part-s
f-g	100	1/s
a	1e+05	1/s
b	8e-14	m^3/part-s
d_p	2.5e-08	m
ρ_{soot}	1800	kg/m^3

A conventional Zeldovich mechanism with partial equilibrium assumptions for the estimation of O and OH radicals concentrations is employed to compute the production of NO_x inside the combustion chamber. Radiation heat transfer was computed using the Discrete Ordinates model.

The definition of parameterized performance indicators in IC engines can be difficult due to the strong interaction between several of the parameters themselves and the implications of changing some of the operating characteristics. In the current work, for instance, changing the number of injection pulses affects primarily the time between the pulses, whose handling is very important in the reduction of pollutant emissions, but it also has an effect on the momentum of each injection pulse, which can be critical in the enhancement of the entrainment of oxygen into the core of the spray. The fundamental objective of the injection pulses is to affect regions of the flame where pollutants are being generated. The appropriate timing of the injection sequence could bring fuel droplets to high-temperature regions where they would evaporate and burn more rapidly. In addition, because of the endothermic nature of the evaporation of the droplets, the local temperature could be reduced sufficiently to provide a reduction in NO_x production. At the same time, the shape of the injection pulse, together with the timing, can significantly affect the momentum of the spray and, as a result, alter the region in which combustion takes place and the amount of oxygen entrained into the fuel rich areas. If these two characteristics can be managed to some extent, then a simultaneous reduction of soot particulates and NO_x would be feasible, in theory.

The numerous challenges that internal engine combustion modelling involves were initially tackled from a perspective in which no major laws of physics or thermodynamics are violated. The simplified approach should help towards the identification of parameters that can help us reach the objectives of a simultaneous reduction of soot and NO_x. In that regard, RNG *k-ε* model was employed to solve for the turbulence field and the main reaction chemistry was computed using a single-step gasoil-air mechanism, the Eddy Dissipation Concept was assumed to account for the turbulence-chemistry interaction.

The engineering rationale behind the current technique is further based on the belief that the delta in the droplet velocity due to pulsing would generate instabilities on the droplet boundary layer. This would in turn lead to the removal of the layer and, as a result, an increased heat transfer between results the two phases yielding enhanced combustion behaviour. The typical droplet lifetime in each one of the cases studied here was computed from equation (4),

$$t_d = \frac{D_p^2}{\beta_b} \tag{4}$$

where β_b is the burning coefficient; a function of the thermodynamic properties of the fuel in liquid phase and the Nusselt number, as described in equations 5 and 6.

$$\beta_b = \frac{4k_g Nu}{\rho_l C_{p,g}} \ln(B+1) \tag{5}$$

$$Nu = 2 + \frac{0.555\,\mathrm{Re}^{1/2}\,\mathrm{Pr}^{1/3}}{\left[1 + \frac{1.232}{\mathrm{Re}\,\mathrm{Pr}^{4/3}}\right]^{1/2}} \tag{6}$$

where k_g is the thermal conductivity of the fuel, ρ_l is the density of the fuel in liquid phase, $C_{p,g}$ is the specific heat capacity. B is normally referred to as the dimensionless Spalding transfer number, and can be calculated using the expression in equation 7.

$$B = \frac{\frac{\Delta h_c}{c} + C_{p,g}(T_\infty - T_s)}{h_{fg}} \tag{7}$$

3. RESULTS

The results presented in this paper represent a continuation of the work done by the authors on excited free jet gas flames [24, 25] as the fuel stream pulsing techniques are applied to practical case scenarios in diesel engines.

One of the initial steps comprised the evaluation of the effects of the start of the injection in the baseline case, i.e. a single pulse injection with a duration of 21 CAD.

The ignition delay is one of the most critical parameters to be taken into account during the design process of a diesel engine and its injection system. Figure 2 depicts the difference observed between a case in which the fuel injection starts at 10 deg BTDC and one where the injection starts at the TDC. The in-cylinder pressures achieved with the injection advance are clearly higher, as the temperature rise due to combustion coincides with the TDC, i.e. minimum volume. This effect is advantageous from the performance viewpoint, but the higher pressures generate larger volumes of pollutants.

The results observed in this study also hint at the importance of the injection timing, as mentioned in the introduction. Whereas the cases with 4-pulses seemed to produce heat release levels comparable to the baseline single pulse and a reduction in soot and NO_x, the higher frequency sequences did not seem to enhance the combustion inside the cylinder and the lower soot and NO_x levels observed are likely to result from the fact that the combustion is not complete and, consequently, the maximum temperature reached inside the combustion chamber is also lower than in the baseline case and the 4-pulse injection, as depicted in figure 3.

An aspect that can significantly help in the analysis of internal engine combustion performance is the evaluation of the thermal efficiency of the cycle, as defined in equation 8. The modifications made to the injection sequence implied that the same crank angle position would not necessarily mean that that the thermodynamic environment was also identical. As a result it was not straightforward to determine the points in the cycle that would serve as a reference. Figure 4 gives a picture of the p-V diagrams for the final part of the compression stroke and the combustion stage, which was used to extract the reference points. It can be appreciated in these graphs that the 4-pulse injections showed higher in-cylinder temperatures in the expansion stroke compared to the other sequences. It is also interesting to note the point at which the maximum temperature is reached inside the combustion chamber. Whereas the 8 and 14-pulse sequences presented the peak temperatures earlier, the 4-pulse cases have delayed this peak further into the expansion stroke. Offsetting the combustion and higher in-cylinder temperatures in the cycle can adversely affect the maximum thermal efficiency, as suggested by the bar chart in figure 5.

$$\eta_{th} = 1 - \frac{1}{r^{\gamma-1}}\left(\frac{\alpha^{\gamma} - 1}{\gamma(\alpha - 1)}\right) \tag{8}$$

where r is the compression ratio $r = \frac{V_1}{V_2}$, and α is referred to as the cut-off ratio, which is the ratio of the volumes at the start and at the end of the combustion process: $\alpha = \frac{V_3}{V_2}$.

The ratio of specific heats, γ, is assumed to take a value of 1.35. The trends suggested by this chart are somewhat in agreement with the observations in engine case scenarios, where a drop in engine performance, caused by lower thermal efficiency, is noted with some stratification sequences of the injection pulse. As depicted in figure 6 the levels of soot emissions are reduced as the frequency of the pulses is increased. On the other hand, identical trends are not necessarily found for each operating regime. The graphs in figure 7 depict the soot concentration inside the combustion chamber at an engine turning speed of 2300rpm. It is interesting to note that the lowest concentration corresponds, as in the previous case, to injections with a higher pulse frequency, but also the fact that the soot emissions with the 4-pulse cases are visibly higher than the baseline. This is probably due to the changes in the flow structure inside the cylinder, which would affect the evaporation of the fuel droplets and the combustion pattern. These results highlight the critical nature of the injection timing in a Diesel engine, where the emission of pollutants can be increased more easily than decreased due to out-of-phase injections.

The temperature contours and the spray droplet size distribution depicted in figure 8 would support the belief that the thermo-fluid processes inside the cylinder of a reciprocating engine vary substantially depending on the engine speed. Variations in turbulence quantities are mainly responsible for much of the differences observed between these two engine speeds. This behaviour is also expected to be very sensitive to the flow around the valves during the intake and exhaust strokes. A few recent CFD studies have modelled IC engines with moving valves. However, this is not widely implemented and, consequently, still implies a degree of uncertainty. In addition, it requires a significant amount of computational resources.

In the analysis of the results, one items of interest was to determine whether there was a relationship between the different timescales involved in the process. The matrix to perform this analysis in a comprehensive manner becomes rather complex when time-dependent variables such as crank speed, evaporation characteristic time, injection sequence, turbulence time scale, ignition delay or reaction time are taken into consideration.

The graphs depicted in figure 9 refer to the change in the ratio between the injection frequency and the turbulent mixing frequency; the latter defined as the inverse of the turbulence time scale, as in equation 2.

$$\varphi = \frac{f_{injection}}{\varepsilon / k}\eta_{th} \tag{9}$$

This equation is intended to identify whether the injection pulses cause a noticeable effect in the turbulence field inside the cylinder. These graphs show that for the highest frequency pulse, the mixing frequency is reduced during the later stages of combustion with respect to the baseline, which could explain why the combustion performance is not as good when higher frequency pulses are employed. On the other hand, this trend is not so clear for the 4-pulse sequences, as it seems that the mixing frequency is similar to the baseline, which, as before, could explain the fact that the 4-pulse sequences were close to the single pulse in terms of combustion performance.

Looking at the curves from the 4-pulse injections, it can be seen that the ratio of frequencies has very similar values up to +10 CAD ATDC, when the mixing frequency for the type-A sequence

remains more or less constant, while it decreases w in the type-B sequence. This can also be appreciated in figure 10, where the turbulent kinetic energy (TKE) and the turbulence dissipation rate (TDR) are plotted separately. In the case of type-B injection, the TKE inside the cylinder enters a plateau whilst it is still rising with type-A. The discrepancy between these two sequences could be due to a difference in the state of the combustion process, as can be deduced from the thermal efficiency charts in figure 5.

On the other hand, a striking conclusion that can be drawn from the current results refers to one of the most critical factors in the combustion process as being due to the start of the combustion. Preparing an optimum pre-combustion environment is essential in order to maximise the outcome of the process. As a result, the shape and sequence between the first two pulses in the series is, in many cases, more important than the sequencing thereafter. For this reason it could be seen that there were equal or even greater differences between types A and B of the 4-pulse sequence than among the different injection patterns simulated. The bar chart in figure 11 depicts the time-averaged fuel evaporation rate for each one of the injection sequences tested in this study. The results are normalized with respect to the single pulse injection. Both 4-pulse options returned higher levels of droplet vaporization, although increasing the pulse frequency from that point on did not result in any further benefits. Nonetheless, it must be appreciated that the 8 and 14-pulse sequences would be comparable to sinusoidal frequencies of 5 and 9kHz respectively, given the 21CAD degree injection period and the engine speed. A pulsating spray with these characteristics represents a major computational challenge on its own and, considering the environment in which the injection takes place, could introduce some numerical inaccuracies in the solution.

The analysis of the droplet lifetime, as depicted in the figures 11 for the normalized droplet evaporation rate and figure 12 for the averaged droplet lifetime, suggest that the pulsing of the fuel injection is effectively achieving a premixed-like combustion stage at the beginning of the injection. This, in turn, raises the temperature during the initial phase, a result , in agreement with what was observed in the in-cylinder temperatures, indicating a slight advance of the combustion process when a pulsing injection was applied. The difference between the different pulses is very small, apart from the 14-pulse sequence, which seemed to predict longer droplet lifetimes towards the end of the injection cycle.

The ratio between the droplet lifetime and the turbulence mixing timescale, as depicted in figure 13, indicates that the limiting process in the combustion process is turbulent mixing. The graphs in this figure reveal that there is a larger value for this ratio during the first 5 CAD, approximately, of the injection stage with the pulse injections than with the baseline. On the other hand, from figure 12, it is known that the droplet lifetime during this small part of the combustion cycle is very similar for all cases, including the baseline. Therefore, the change in the ratio is caused by a decrease in turbulence time scale, hence suggesting that the pulsing might not offer a great improvement in droplet evaporation rates, but instead appears to enhance the gaseous phase mixing. These results would be in agreement with the previously published study by the authors on jet flames, where the mixing between fuel and oxidizer streams was enhanced by the pulsing of the fuel inlet. In the case of the liquid fuel injection in an IC engine presented here, the models available to simulate the discrete phase are unable to capture the effects of fuel stream fluctuations on the development of the boundary layer around the droplets. We suspect that this effect would play an important role in the determination of the corresponding heat and mass transfer rates from the droplet into the surroundings and that the fluctuations in the fuel inlet stream would cause a reduction in the thickness of the boundary layer around the droplets and, as a result, enhance the heat and mass transfer rate between the two phases.

As stated previously, the initial objectives in this preliminary study was to determine whether there would be any advantages derived from the pulsing in the mixing of the gaseous species, assuming that the evaporation rates would not be directly affected by the pulsing.

The data points depicted in figure 14 plot the soot concentration against the NO_x concentration for each case, where the emissions are better as the data points get closer to the origin.

As mentioned earlier, it is nonetheless important to consider all of the relevant data available for a specific case. For example, if figure 14 is analyzed independently, one would arrive at the conclusion that the optimum solution, amongst the ones studied herein, are the higher pulse frequencies. However, it was shown in figure 3 that the combustion performance, as judged by the flame temperatures, is lower with the 8 and 14-pulse sequences.

CONCLUSIONS

In the case studies presented in this paper, it was difficult to establish a relationship between the turbulence level changes caused by the different pulses of the injection and the emissions reductions. In the area of diesel engines, the performance of combustion is highly dependent on the initial injection environment, which, in this case could overshadow the effect generated by other parameters.

In any case, there appears to be an interaction between the number pulses applied to the injection sequence and the combustion performance and pollutant emissions. However, it is still unclear whether this is due to the effects caused during the pre-combustion stage –dwell between first and second injections- or the non-premixed diffusion flame stage.

At present we are continuing the work and trying to isolate the effects inasmuch as possible by maintaining a constant pre-combustion stage and investigating a number of injection sequence options during the diffusion stage.

LIST OF FIGURES

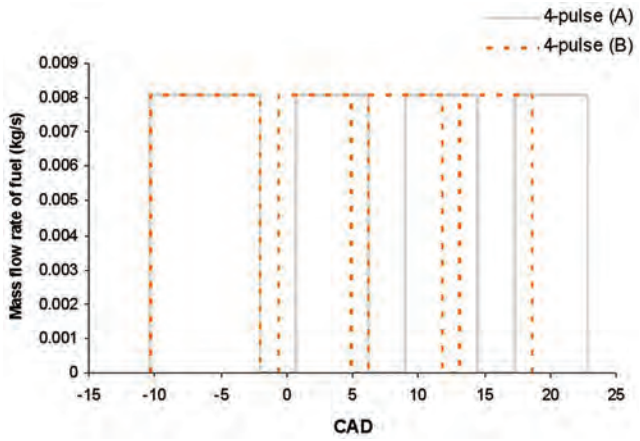

Fig. 1. Difference between modes A and B in 4-pulse sequence

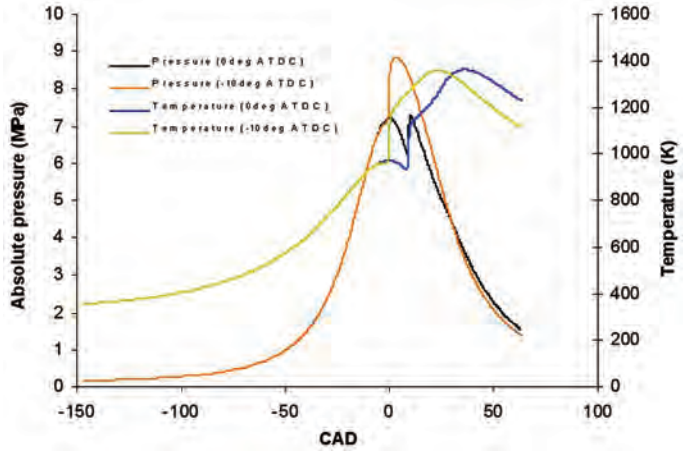

Fig. 2. SOI effect on in-cylinder parameters

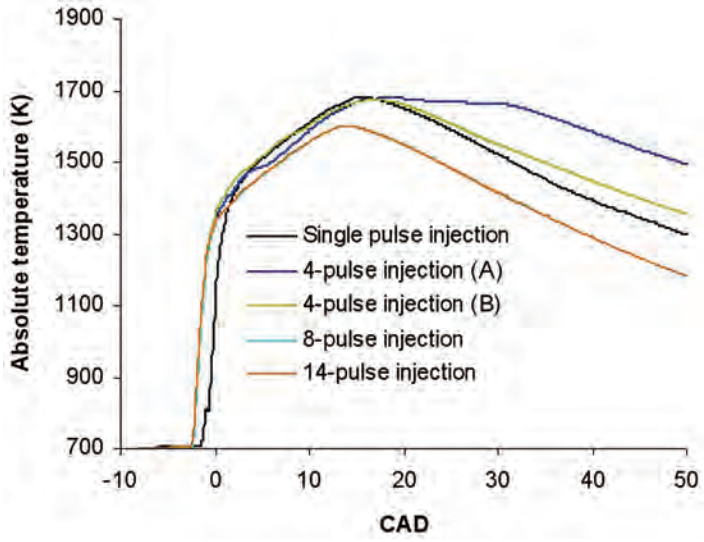

Fig. 3. In-cylinder temperature during combustion stage

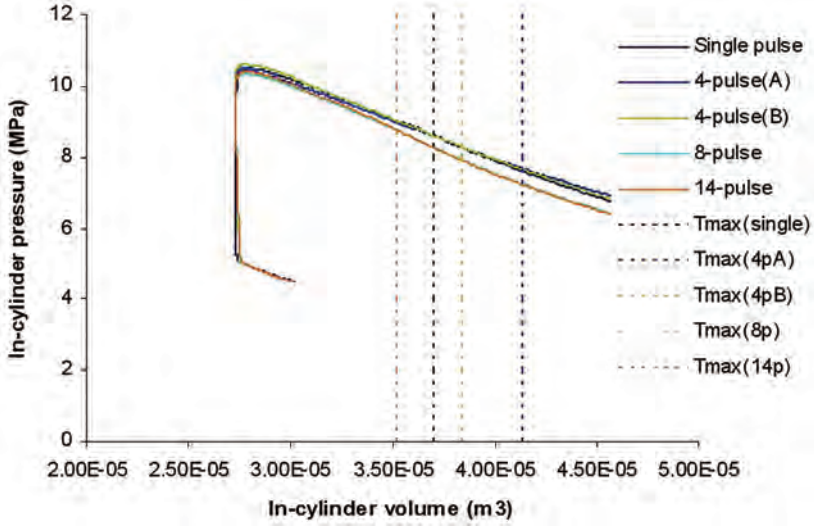

Fig. 4. Cycle p-V diagram during combustion stage

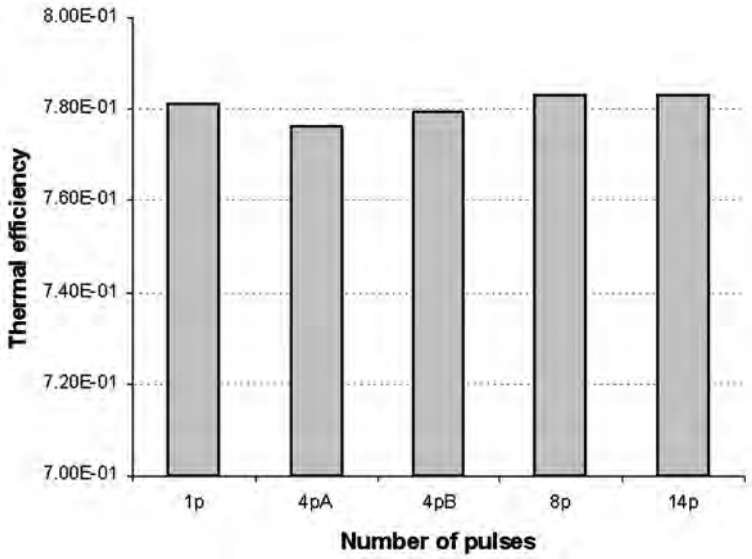

Fig. 5. Thermal efficiency of combustion stage

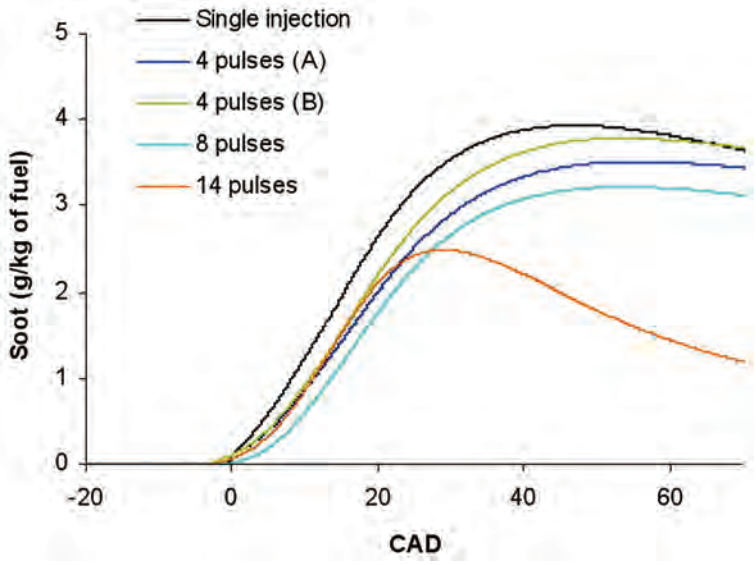

Fig. 6. In-cylinder soot concentration at 1600rpm

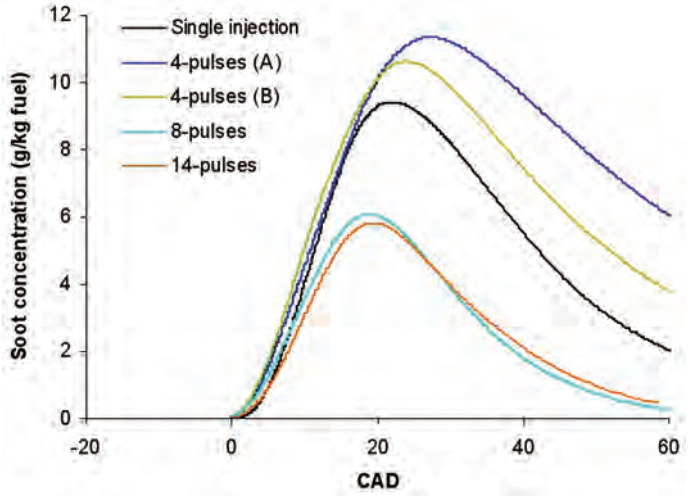

Fig. 7. In-cylinder soot concentration at 2300rpm

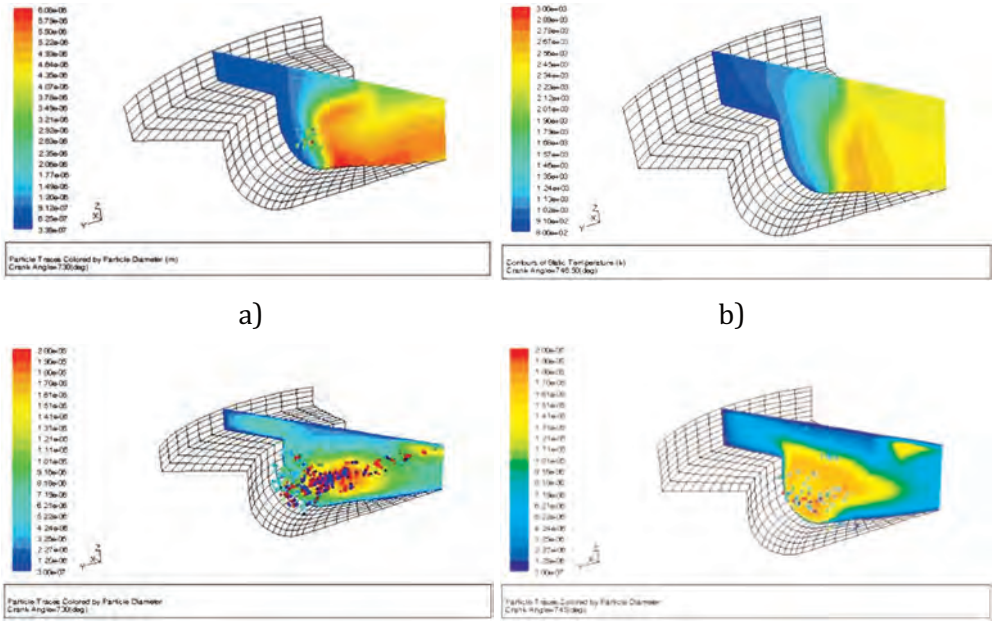

a) b)

c) d)

Fig. 8. Temperature contours and fuel droplet visualization by droplet size at 730 CAD and 745 CAD for engine speeds 1600rpm (a and b) and 2300rpm (c and d)

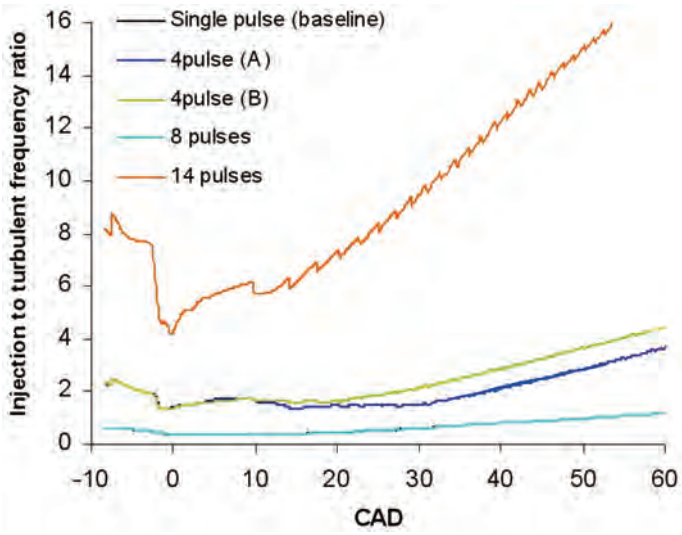

Fig. 9. Comparison of ratio of injection and turbulence frequencies

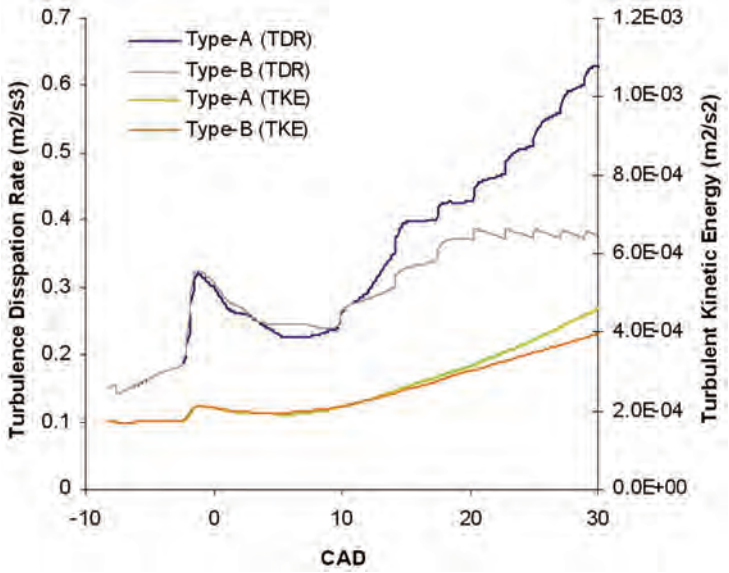

Fig. 10. Turbulent kinetic energy and turbulence dissipation rate or 4-pulse injection sequences

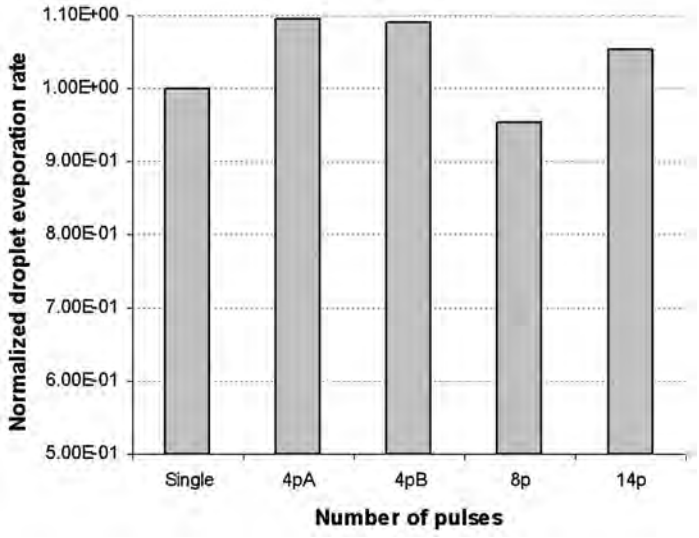

Fig. 11. Cycle-averaged droplet evaporation rate normalized with respect to the single pulse case

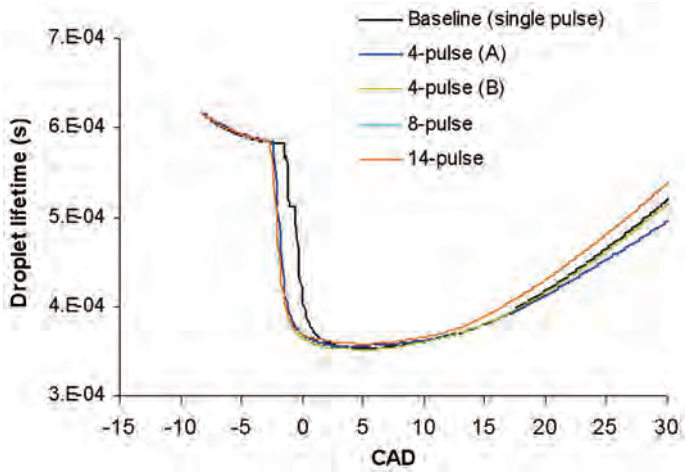

Fig. 12. Computed droplet lifetime during combustion process

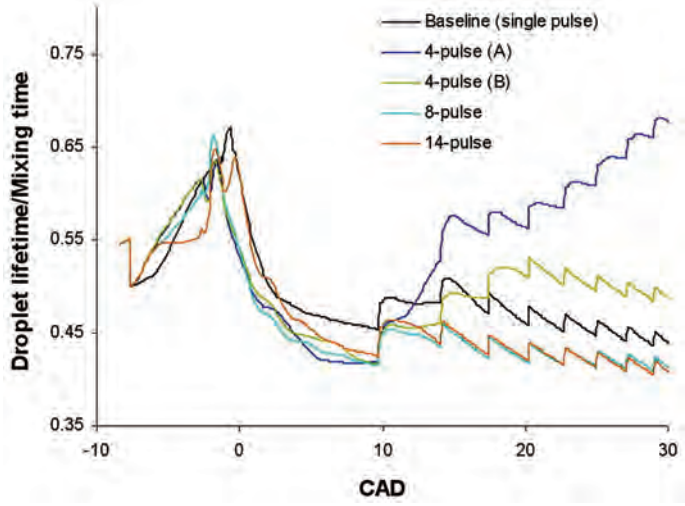

Fig. 13. Ratio between the computed droplet lifetime and the mixing time scale

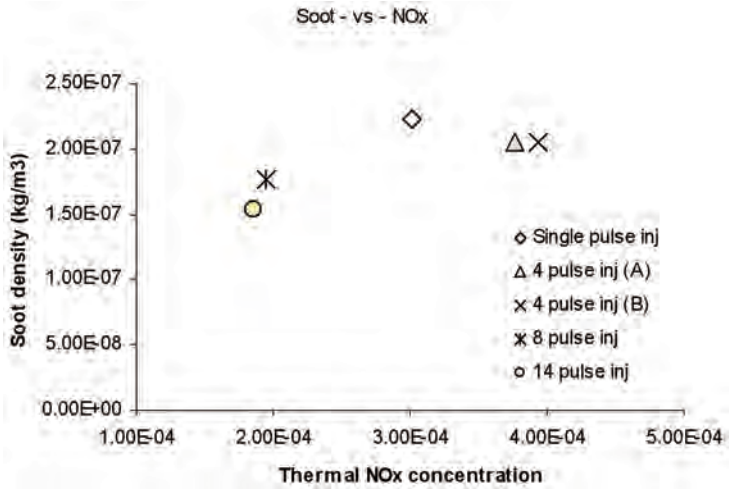

Fig. 14. Relationship between soot and thermal NO_x production with each one of the injection sequences

REFERENCES

[1] Longwell, J.P. "Polycyclic aromatic hydrocarbons and soot from practical combustion engines", In Lahaye, J. and Prado, G. (Eds) Soot Combustion Systems and its Toxic Properties, Plenum Press, New York. pp. 37-57, 1981.

[2] Boyland, E. "The Toxicology of Soot". In Lahaye, J. and Prado, G. (Eds) Soot Combustion Systems and its Toxic Properties, Plenum Press, New York. pp. 13-24, 1981.

[3] Farrell, P.V. and Rajalingam, B. "The Effect of Injection Pressure on Air Entrainment into Transient Diesel Sprays", SAE Technical Paper 1999-01-0523, 1999.
[4] Ayoub, N.S. and Reitz, R.D., "Multidimensional Modeling of Fuel Composition Effects on Combustion and Cold Starting in Diesel Engines" SAE Technical Paper 952425, 1995.
[5] Stephenson, P.W. and Rutland, C.J "Modeling the Effects of Valve Lift Profile in Intake Flow and Emissions Behaviour in a DI Diesel Engine", SAE Technical Paper 952430, 1995.
[6] Reitz, R.D and Rutland, C.J., "Development and Testing of Diesel Engine CFD Models" Prog. Energy Combust. Sci., Vol. 21, pp173-196. 1995.
[7] Curtis, E.W., Uludogan, A. and Reitz, R.D. "A New High-Pressure Droplet Vaporization Model for Diesel Engine Modeling", SAE Technical Paper 952431, 1995.
[8] Kong, S.C., Han, Z and Reitz, R.D. "Development and Application of a Diesel Ignition and Combustion Model for Multidimensional Engine Simulation" SAE Technical Paper 950278, 1995.
[9] Kong, S.C., Rutland, C.J and Reitz, R.D. "Development of an Integrated Spray and Combustion Model for Diesel Simulations" Conference Proceedings Thiesel 2000: Thermofluidynamic Processes in Diesel Engines, 2000.
[10] Barths, H, Antoni, C. and Peters, N., "Three-Dimensional Simulation of Pollutant Formation in a DI Diesel Engine Using Multiple Interactive Flamelets", SAE Technical Paper 982459, 1998.
[11] Pistch, H., Barths, H. and Peters, N. "Three-Dimensional Modeling of NOx and Soot Formation in DI-Diesel Engines Using Detailed Chemistry Based on the Interactive Flamelet Approach", SAE Technical Paper 962057, 1996.
[12] Bai, X. S., Balthasar, M., Mauss, F. and Fuchs, L. "Detailed Soot Modeling in Turbulent Jet Diffusion Flames", 27th Symp. (int.) on Combustion, The Combustion Institute, pp.1623-1630, 1998.
[13] Mauss, F., Schäfer, T., Bockhorn, H. and Rosner, D.E. "Inception and Growth of Soot Particles in Dependence on the Surrounding Gas Phase", Combustion and Flame, Vol. 99, pp. 697, 1994.
[14] Imaoka, R.T and Sirignano, W.A. "A Generalized Analysis for Liquid-Fuel Vaporization and Burning" Int. Journal of Heat and Mass Transfer, Vol. 48, pp 4342-4353, 2005.
[15] Ahn, S.K., Kanimoto, T., Matsui, Y. Matsuoka, S. "Measurement of Flame Temperature in a DI Diesel Engine by Means of Image Analysis of Nega-Color Photographs", Proc. 1st Japan Society of Automotive Engineers − Japan Society of Mechanical Engineers, 1981.
[16] Magnussen B.F "On the Structure of Turbulence and Generalized Eddy Dissipation Concept for Chemical Reaction in Turbulent Flow" 19th AIAA Science Meeting, St Louis, Missouri, USA, 1981.
[17] Tesner, P.A., Snegiriova, T.D. and Knorre, V.G. "Kinetics of Dispersed Carbon Formation", Combustion and Flame, Vol. 17, pp. 253-265, 1971.
[18] Tesner, P.A. Tsygankova, E.I., Guilazetdinov, L.P., Zuyev, V.P. and Loshakova, G.V. "The Formation of Soot from Aromatic Hydrocarbons in Diffusion Flames of Hydrocarbon-Hydrogen Mixtures", Combustion and Flame, Vol. 17, pp. 279-291, 1971.
[19] Kolmogorov, A.N. "A Refinement of Previous Hypotheses Concerning the Local Structure of Turbulence in a Viscous Incompressible Fluid at High Reynolds Number", Journal of Fluid Mechanics, Vol. 13. pp. 82-85, 1962.
[20] Arpaci, V.S. "Microscales of Turbulent Combustion", Prog. Energy Combust. Sci, Vol. 21, pp 153-171, 1995.
[21] Magnussen, B.F. and Hjertager, B.H "On Mathematical Modeling of Turbulent Combustion with Special Emphasis on Soot Formation and Combustion", Proc. Combust. Instit. , Vol.16, pp719-728, 1976.
[22] Magnussen, B.F., Hjertager, B.H., Olsen, J.G. and Bhaduri, D., "Effect of Turbulence Structure and Local Concentrations on Soot Formation and Combustion in C2H2 Diffusion Flames" Proc. Combust. Instit. Vol 17, pp1383-1391, 1979.

[23] Singh, J., Balthasar, M., Kraft, M. and Wagner, W. "Stochastic Modeling of Soot Particle Size and Age Distributions in Laminar Premixed Flames", Proc. Combust. Instit. Vol. 30, pp. 1457, 2005.
[24] López-Parra, F. and Turan, A. "Computational Study on the Effects of Non-Periodic Flow Perturbations on the Emissions of Soot and NO_x in a Confined Turbulent Methane/Air Diffusion Flame" Combust. Sci. and Tech, Vol.179. pp 1361-1384. July 2007.
[25] López-Parra, F and Turan, A. "Computational Study on the Effect of Turbulence Intensity and Pulse Frequency in the Soot Concentration in an Acetylene Diffusion Flame". Int. Conference on Computational Sciences, pp120-128, LCNS 3516, Springer-Verlag, 2005.
[26] Srivatsa, S.K. NASA-Lewis Research Center, NAS3-22542, NASA CR-167930, Garrett 21-4309, 1982.

Fernando Lopez-Parra

NUMERYCZNE BADANIE WPŁYWU UWARSTWIENIA ŁADUNKU DLA WTRYSKU SEKWENCYJNEGO NA EMISJĘ SADZY I TLENKÓW AZOTU DLA SILNIKA O SPALANIU WEWNĘTRZNYM Z ZAPŁONEM SAMOCZYNNYM

Streszczenie

Praca zawarta w niniejszej publikacji stanowi końcowy etap przewodu doktorskiego, gdzie wyniki z badań wydobywających się z dyszy płomieni były zastosowane do typowego wysokoprężnego silnika spalinowego, w celu oceny czy jest możliwy do uzyskania podobny wynik badań. W tej części badań wykonywane były numeryczne badania symulacyjne nad wpływem rozłożonego w czasie wtrysku paliwa dla silnika wysokoprężnego z wtryskiem bezpośrednim. Praca ta ma na celu zbadanie przez autorów praktycznego wykorzystania wyników dotychczasowych prac, gdzie w dyfuzyjnym płomieniu turbulentnym za pomocą pulsacji strumienia paliwa została osiągnięta jednoczesna redukcja NOx i sadzy. Wykorzystany w niniejszym opracowaniu model sadzy jest oparty o koncepcję wirów rozproszonych Magnussena, co stanowi etap pośredni między modelami empirycznymi i modelami fenomenologicznymi, jak i obejmuje on w małej skali efekt turbulencji przy tworzeniu i spalaniu sadzy, ale nie jest oparty na wieloetapowych mechanizmach reakcji. Przedstawione niniejszym wyniki mają na celu uchwycenie realistycznych trendów w tworzeniu się sadzy, trendów które są oparte na rzeczywistych zjawiskach fizycznych, a więc mogą służyć jako podstawa do bardziej szczegółowych prac rozwojowych. Geometria została oparta na uproszczonym jednocylindrowym bezzaworowym przekroju 60-stopniowego silnika Caterpillar 3406 do maszyn ciężkich. Do rozwiązania problemu w obszarze turbulencji został wykorzystany model RNG k-ε a chemię głównych reakcji rozwiązano za pomocą jednokrokowego mechanizmu: olej napędowy-powietrze, podczas gdy do przewidywania wyników wzajemnego oddziaływania turbulencji i chemii została wykorzystana koncepcja rozpraszania wirów a dyskretny model współrzędnych wykorzystano do oceny promieniowania. Wyniki wykazały że istnieje silne oddziaływanie pomiędzy sekwencją impulsów i rozwojem procesu spalania, chociaż trudno jest ocenić czy różnice te wynikają z oddziaływania pomiędzy dwoma pierwszymi impulsami w dowolnej sekwencji czy też w samej sekwencji impulsów.

Przewiduje się że sekwencja 4 impulsów wtrysku spowoduje zmniejszenie emisji sadzy, aczkolwiek utrzyma wyższą temperaturę w cylindrach podczas suwu rozprężania, która to zwiększa wydzielanie NOx. Badania przeprowadzono w dwóch obszarach pracy silnika: 1600 i 2300 obr/min, a pomiędzy tymi obszarami uwidaczniają się niektóre istotne różnice w strukturze i rozwoju płomienia.